Dynamic Properties and PWP-model Parameters of Sandy Soil for Ground Response Analysis

Shiv Shankar Kumar[1], A. Murali Krishna[2] and Arindam Dey[3]

[1] Assistant Professor, School of Civil Engineering, Kalinga Institute of Industrial Technology Bhubaneswar, Odisha, India - 751024, Email: shivshankar.mit@gmail.com

[2] Associate Professor, Department of Civil and Environmental Engineering, Indian Institute of Technology Tirupati, Andhra Pradesh, India – 517506, E-mail: amk@iittp.ac.in

[3] Associate Professor, Department of Civil Engineering, Indian Institute of Technology Guwahati, Guwahati, Assam, India – 781039, Email: arindamdeyiitg16@gmail.com

Abstract. Seismic design of any structures require the dynamic characteristics (modulus degradation and damping variation) of underlying soil in order to incorporate the soil structure interaction effects, and such dynamic behaviour is different for different soils. But, due to unavailability of the site-specific or region-specific dynamic soil properties, geotechnical engineers are forced to use existing dynamic properties curves, which has been developed for other regions. This paper presents the dynamic properties of Brahmaputra sand over wide strain range (0.001% to 5%) based on extensive laboratory tests. Cyclic triaxial apparatuses have been utilized to obtain the required soil parameters along with the liquefaction potential of the soil at different testing conditions (shear strains, confining stresses and relative density). Resonant column tests data have also been added with the cyclic triaxial tests to prove the wide range of strain dependent dynamic soil properties. Results are presented in terms of normalized modulus curves and damping curves, which can be directly utilized for performing any ground response studies in this region. Furthermore, a pore pressure model parameters are provided based on the test data to perform non-linear effective stress ground response studies with PWP dissipation/generation.

Keywords: Dynamic properties, Low and high shear strains, Liquefaction, PWP-model Parameters, Cyclic triaxial tests.

1 Introduction

The Northeastern India, located close to the Himalayan seismic belt, experience moderate (moment magnitude, $Mw \leq 6.0$) to large earthquakes ($6.0 < Mw \leq 8.0$) very often. This region also has witnessed two great earthquakes ($Mw > 8.0$) one each in 19th and 20th centuries (Kayal [1]), see Fig. 1. The past seismic events also lead to wide spread liquefaction in this region especially during 1897 Shillong earthquake and 1950 Assam earthquake [2, 3]. Researchers predict that this region is due to a large impounding earthquake in the near future [4]. Figure 1 presents the tectonic

setup map of Northeast India superposed with seismic events (Mw≥6.0) since 1897. As it is impossible to predict, warn or prevent the occurrence of these natural calamities, the way forward in reducing the impact is through better preparedness by having efficient aseismic design of infrastructure especially for lifeline structures like bridges, dams, etc. Some of these structures were built much before the seismic codal developments in India and hence, researchers have initiated requalification studies of such structures [5-7].

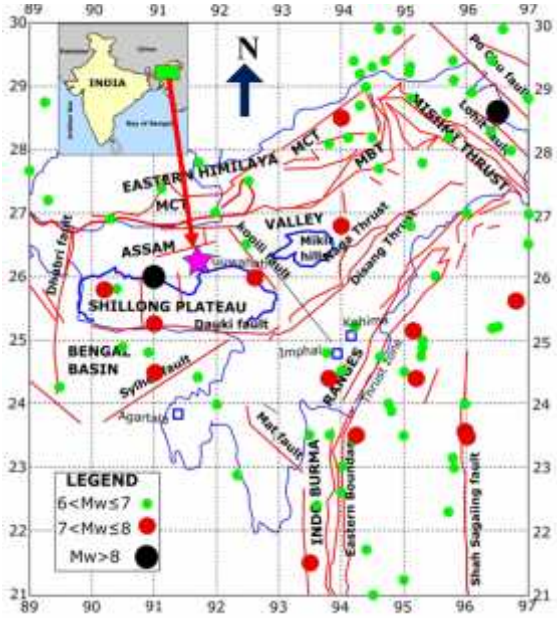

Fig. 1. Seismotectonic map of Northeast India (after Raghu Kanth [3])

It is very well recognized that underlying soil plays a crucial role in evaluating the stability of the overlying structure. The response of soil to each earthquake is unique depending upon strength and stiffness properties of the soil and also on the parameters of exciting motion. Some earthquakes can induce very small strains in the soil, while some could trigger significant strains which can mobilize the entire shear strength of soil. Hence, the strength of soil with varying strains (shear modulus, G and Damping ratio, D) is required to perform an aseismic design of structures. Researchers have proposed such strain dependent dynamic soil properties based on extensive experimental and analytical relationships [8-12]. The application of such empirically obtained strain dependent properties is often unreliable and being questioned. Based on these observations, the article is organized in to two folded, in order to obtain the strength and stiffness of the soil of this highly active seismic region.

- The dynamic characterization of chosen sand was obtained using high quality element testing techniques (Cyclic Triaxial, CTX) at different loading conditions (varying shear strain levels, confining stresses and initial void ratios).
- The liquefaction potential of Brahmaputra Sand (BS) was estimated using extensive strain controlled CTX tests. The results are presented in terms of Pore Water Pressure (PWP)-model parameters to perform non-linear seismic Ground Response Analysis (GRA) incorporating liquefaction phenomena.

2 Experimental Program

2.1 Material

BS was soil collected from Brahmaputra River near Guwahati region, Assam (India). The particle size distribution of the sand combined with probable liquefiable zones for sandy soils is shown in Fig. 2, which confirms that BS is highly susceptible to liquefaction. Index properties of the soil were determined according to the ASTM standards and are presented in Table 1. The soil has been classified as poorly graded sand (SP) according to Unified Soil Classification System.

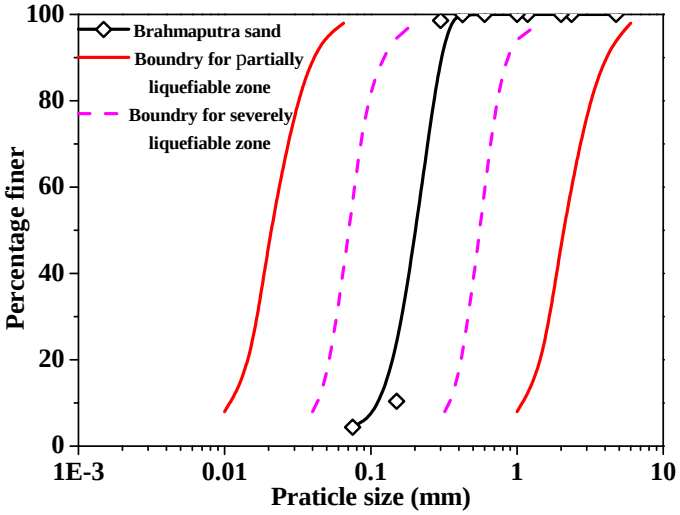

Fig. 2. Particle size distribution of BS compared with liquefiable soil zones

Table 1 Index properties of sand

Soil descriptions	values	Code followed
Mean grain size, D_{50} (mm)	0.21	[13]
Minimum unit wt. (kN/m^3)	13.85	[14]
Maximum unit wt. (kN/m^3)	16.84	[15]
Uniformity coefficient (C_u)	1.47	

Coefficient of curvature (C_c)	1.09	
Specific gravity	2.7	[16]
Classification symbol	SP	[17]

2.2 Sample preparation and testing procedures

In order to obtain the strain dependent dynamic soil properties (G and D), CTX apparatus have been utilized as one single equipment cannot provide G and D variation over the required strain range (0.001% to 5%). Sample preparation and testing procedure of CTX tests were followed according to the standards, ASTM [18] and ASTM [19], respectively and are described in detail by Kumar et al. [19], respectively. Tests are aimed to evaluate the dynamic soil properties at varying effective confining stress (σ'_c) and varying relative densities (D_r). The summary of the testing program is listed in Table 2.

Table 2 Investigating parameters for CTX tests

Test	D_r (±2%)	e	σ'_c (kPa)
CTX	30 (e_{target}=0.860)	0.868	50
		0.856	100
		0.863	150
	60 (e_{target} =0.758)	0.765	50
		0.746	100
		0.741	150
	90 (e_{target} =0.656)	0.667	50
		0.672	100
		0.650	150

3 Results and discussions

CTX tests have been used to evaluate the shear modulus and damping ratio of BS for high shear strain range i.e. from 0.01% to 5%. The typical stress strain behavior of a cyclically loaded soil is expected to follow the hysteresis loop and was observed to be asymmetrical (Fig. 3) at shear strains greater than 0.15% [20]. This high-strain (>0.01%) dynamic properties of cohesionless soil was taken from Kumar et al. [20].

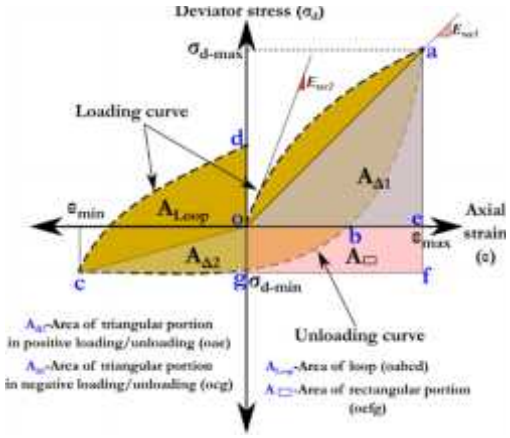

$$E = \frac{E_{sec1} + E_{sec2}}{2}$$

$$G = E/[2(1+\text{³})]$$

¥ = (1+ ³)£

$$D = \frac{1}{\text{®}} \times \frac{A_{L(o-a-b-c-d)}}{A_{\Delta 1} + A_{\Delta 2} + A}$$

Fig. 3. A typical asymmetrical hysteresis loop (after Kumar et al. [20])

3.1 Comparison of BS results with other Indian sandy soil data

Figure 4 present the variations of G/G_{max} and D for wide range of γ (evaluated using both RC and CTX) at different σ'_c and D_r. Figure 4a compares G/G_{max} of BS with G/G_{max} curves suggested in literatures [8, 10, 11]. Seed and Idriss [8] provided broad range of G/G_{max} curve for sand, which is commonly used in GRA due to the lack of site-specific data [21-23]. Dammala et al. [24] have conducted the resonant column tests on dry cohesionless soil up to γ = 0.1%, it is not practically justified to use this results of strain range 0.0001% to 0.1%, in case of saturated sand. It was reported in the literature [25-27], that the shear strain of 0.01% is a limiting value of volumetric threshold shear strain below which no significant pore water pressure is generated in the saturated cohesionless specimen. Therefore, the consideration of low-strain dynamic properties of soil up to γ = 0.01% will not violate the assumption that the dynamic properties of dry and saturated cohesionless soil up to 0.01% are nearly same. It is also seen that the RC and CT data of BS soil does not fall in range proposed by Seed and Idriss [8] and Ishibashi and Zhang [10] while consistent with Darendeli [11] curves at high strains.

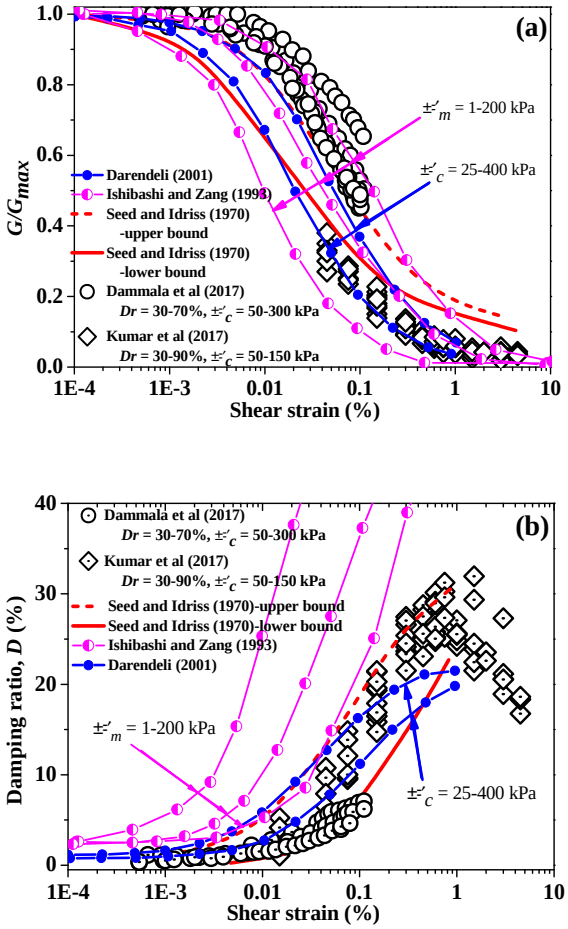

Fig. 4. Variations of (a) G/G_{max} and (b) D with γ from RC and CT tests at different σ'_c and D_r

Figure 4b describes D of the BS soil obtained from RC and CT tests, and compared with the above discussed traditional curves. It can be seen that both RC and CTX data up to γ = 1%, falls in the lower range of Seed and Idriss [8] curve beyond which D decreases. It can also be observed from Fig. 4b, that the Ishibashi and Zhang [10] shows significantly higher damping than the estimated damping values, whereas Darendeli [11] shows the lower values of damping at shear strains greater than 0.2%. Figure 5 present the variations of G/G_{max} (Fig. 5a) and damping 'D' (Fig. 5b) with shear strain for sands of Indian region. The data other than BS soil was taken from the mentioned literatures in Fig. 5. A range in terms of lower and upper bound is provided for G/G_{max} curve in which all Indian sands accommodate. This upper and lower bounds of G/G_{max} and D of Indian sands can be useful for the many site-specific engineering applications such as seismic GRA and stiffness calculations of foundations.

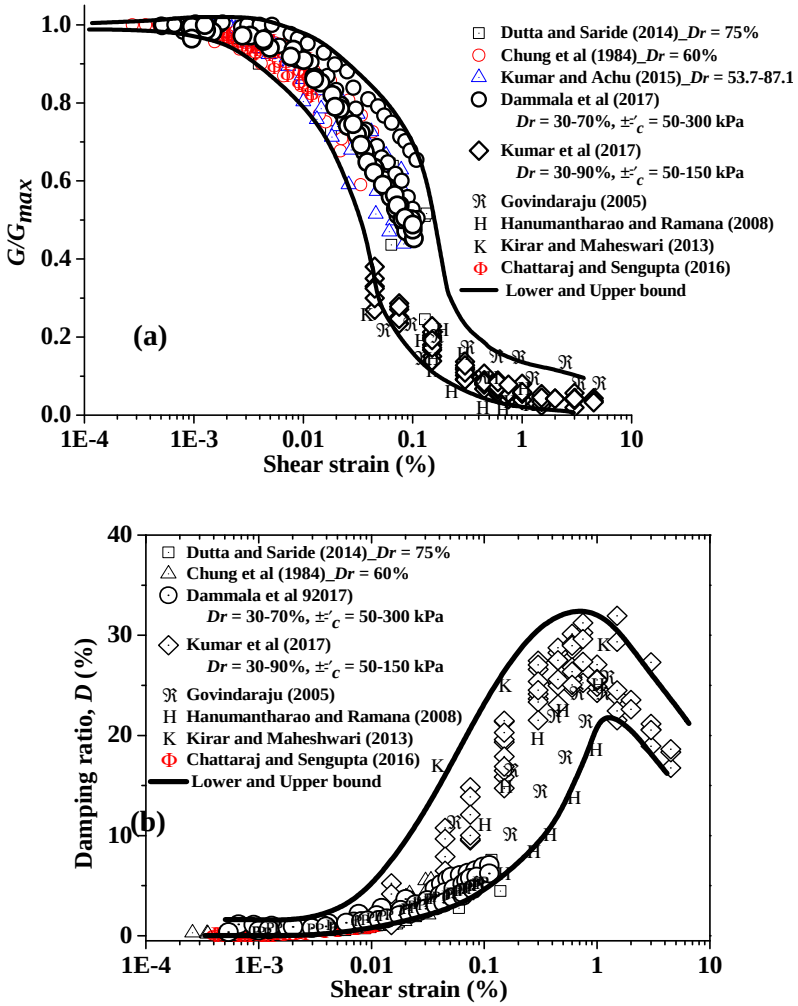

Fig. 5. Variations of (a) G/G_{max} and (b) Damping ratio with shear strain for Indian sandy soils

3.2 Liquefaction analysis based on cyclic triaxial tests

Liquefaction is often represented using pore water pressure ratio (r_u), which is the ratio of excess pore pressures (Δu) generated in the soil column to the mean effective confining stress (σ'_c). Figure 6a presents the variation in maximum r_u in each cycle with N at different γ. It shows that with the increase in γ, i.e. from 0.045% to 0.75%, the liquefaction resistance decreases. The r_u value was observed to be nearly 0.2, 0.55, 0.95, 1, 1, 1 and 1 at γ = 0.045%, 0.075%, 0.15%, 0.30%, 0.45%, 0.60% and 0.75%, respectively. The BS specimen, prepared at D_r = 30% and subjected to σ'_c = 100 kPa, attains $r_u \geq 0.90$ in 1st cycle for γ ≥ 0.75%. It can also be noted that more number of cycles (N) are required to initiate liquefaction for soil specimen subjected

to γ less than 0.60%. Similar responses were observed for the specimen prepared at D_r = 60% and 90% when soil specimens subjected to σ'_c = 50 kPa and 150 kPa.

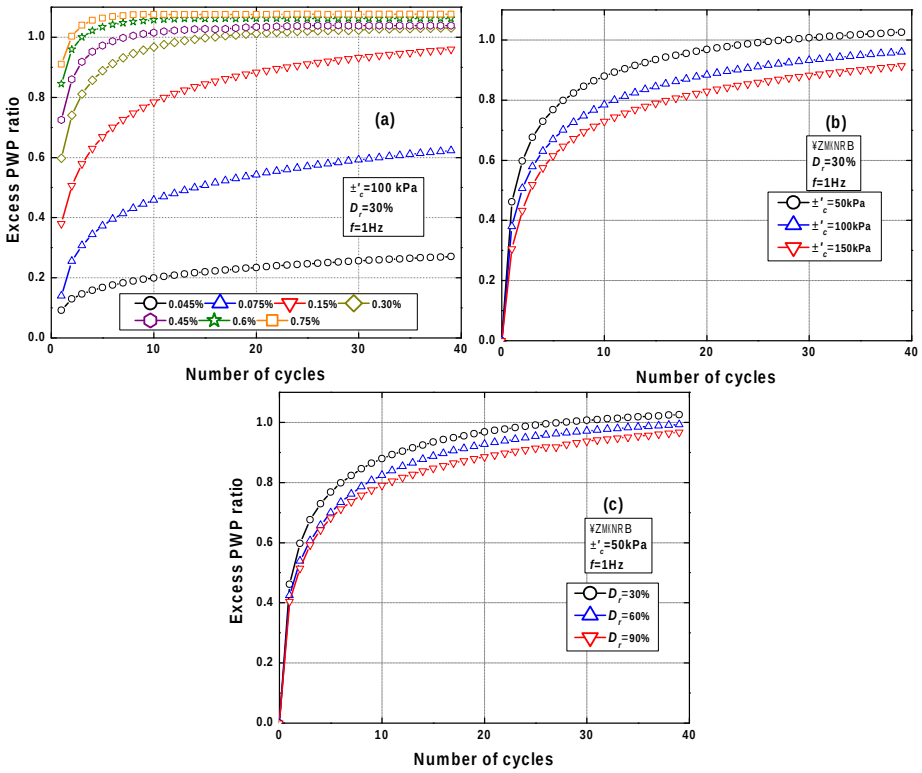

Fig. 6. Variation of r_u with N at different (a) γ (b) σ'_c and (c) D_r

Figure 6b presents the variations of r_u at different σ'_c for BS specimens prepared at D_r = 30%. It also shows the variations of r_u at γ = 0.075% and 0.15%. For γ = 0.075%, maximum r_u value is 0.8 at σ'_c = 50 kPa, while it is 0.53 at σ'_c = 150 kPa, whereas for γ = 0.15%, the maximum r_u value reached 1 at 30 cycles for σ'_c = 50 kPa, while r_u = 0.90 at 30 cycles for σ'_c = 150 kPa. Thus, the figure indicates that for a given shear strain value and number of cycles, the r_u values decreased with increase in σ'_c. It also shows that, for identical number of cycles (N) and σ'_c, the tendency to liquefy the specimen increases with increase of γ.

Figure 6c illustrates the variation in r_u for test specimens prepared at different D_r i.e. 30%, 60% and 90% and tested at σ'_c = 50 kPa with γ of 0.075% and 0.15%. It reflects that the r_u decreases with the increase of D_r for a constant γ and σ'_c. At γ = 0.075%, the BS specimen shows maximum r_u = 0.8 and 0.7 at 40 cycles, for D_r = 30% and 90%, respectively, whereas at γ = 0.15%, the maximum r_u was observed to be 1.0 (at 32 cycles) and 0.9 (at 40 cycles), for D_r = 30% and 90%, respectively. Therefore, it can be stated that the initiation of liquefaction is significantly affected by D_r as well as γ. It is also seen that for any constant γ (0.075% or 0.15%), the r_u is nearly same at first cycles for all three D_r.

3.3 Determination of PWP-model parameters

Pore water pressure (PWP) models simulate the generation and dissipation of excess pore pressures during cyclic loading. Numerous PWP models, ranging from simple to complex nature, are available in the literature [28-33]. However, to perform non-linear effective stress analysis, commercial programs such as DEEPSOIL [25], employ extended Dobry et al. [31] PWP model as the required input parameters can be efficiently obtained by performing stress/strain controlled CTX/DSS tests on saturated soil samples. Based on the strain-controlled CTX tests on sandy soil, Vucetic and Dobry [26] extended the basic PWP model developed by Dobry et al. [31] in Eqn. (1). The model emphasizes the generation of PWP with number of cycles and applied cyclic shear strain.

$$r_{u,N} = \frac{p.N.F.(¥ - ¥_t)^S}{1 + N.F.(¥ - ¥_t)^S} \tag{1}$$

where $r_{u,N}$ = excess PWP ratio at N number of cycles; γ = cyclic shear strain amplitude; p, F and s are the curve fitting parameters; and γ_t is the threshold shear strain below which no significant PWP is generated or shear strain below which no significant permanent volume changes are observed (also called volumetric threshold shear strain). Traditionally, the value of γ_t is established from laboratory tests on saturated samples [34]. However, as the CTX tests were conducted at high strains and RC tests were performed in dry conditions, the value of γ_t was established at a G/G_{max} value of 0.80 as suggested by Vucetic [34]. The magnitude of γ_t increases with increasing confining pressure which means that the depth of overburden increases the strain required for the volume changes or significant pore pressure generation. Therefore, for the three tested confining pressures (50, 100 and 150 kPa), the values of γ_t established are 0.02%, 0.03% and 0.035% respectively. The proposed γ_t values are consistent with the literature suggested range for sands -0.01% to 0.04% [35-37].

The PWP model curve fit parameters (p, F and s) are obtained by performing regression analysis on the experimental data for the three considered σ'_c values using the Eqn. 7. As described, the effect of relative density is insignificant in the PWP generation (Fig. 6c) and hence the same is neglected in the analysis. Figure 7 depicts the obtained results of PWP model with the fitting parameters, at three σ'_c values. Since, the dynamic properties (shear modulus and damping ratio) of BS was evaluated for the first cycle (N = 1), the fitting parameters of the PWP model have also been evaluated for the first loading cycle (N = 1).

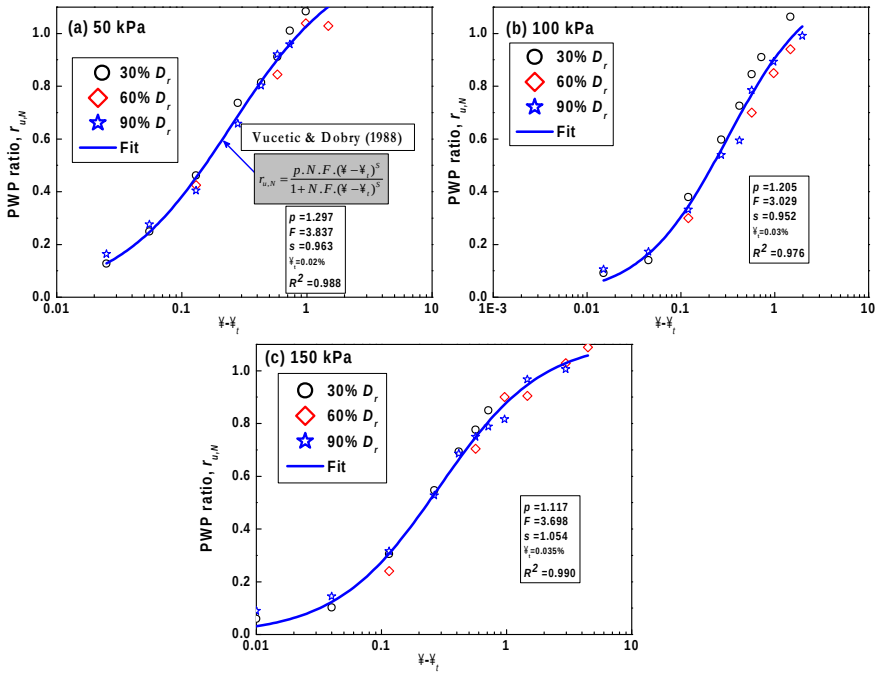

Fig. 7. Pore water pressure ratio variation of BS at (a) 50 kPa, (b) 100 kPa and (c) 150 kPa effective confining pressure

4 Conclusions

In this study, cyclic triaxial tests data at different testing conditions are presented to characterize the dynamic behaviour of BS soil. Based on the cyclic triaxial tests at higher shear strains, the following conclusions were drawn:

1. Shear modulus degradation and damping ratio for wide range of shear strain i.e. from 10-4 % to 5% has been compared with existing material models, which emphasize the importance of site-specific dynamic properties of Indian sandy soil.
2. PWP variation in cyclic triaxial reflects that the r_u decreases with the increase of D_r means at higher D_r, higher N_c are required to liquefy the soil specimens for a constant γ and σ'_c. The r_u significantly decreases with the increase of σ'_c whereas, the same is marginally affected, which can be neglected, by D_r for first loading cycles.
3. Further, PWP parameters p, F, and s for BS soil, required for the effective stress GRA with PWP generation/dissipation studies, have been estimated using the nonlinear curve-fitting technique.

Therefore, the obtained wide strain range dynamic soil properties along with PWP-model parameters will be highly useful in performing non-linear effective stress GRA studies, in Northeast India, incorporating the pore pressure generation and dissipation in the soil column.

References

1. Kayal, J.R., De, R.: Microseismicity and Tectonics in Northeast India. Bulletin of Seismological Society of America 81:131–138 (1991).
2. Oldham, R. D.: Report of the great earthquake of 12th June, 1897. Office of the Geological survey, (1899).
3. RaghuKanth, S. T. G., Dash, S. K.: Evaluation of seismic soil-liquefaction at Guwahati city. Environmental Earth Science 61, 355–368 (2010).
4. Khattri, K. N.: Probabilities of occurrence of great earthquakes in the Himalaya. In Proceedings of Indian Academic, Science Earth Planet Science 108, 87–92 (1992).
5. Dammala, P. K., Bhattacharya, S., Krishna, A. M., Kumar, S. S., Dasgupta, K.: Scenario based seismic re-qualification of caisson supported major bridges - A case study of Saraighat Bridge. Soil Dynamics Earthquake Engineering 100, 270–275 (2017a).
6. Krishna, A. M., Bhattacharya, S., Choudhury, D.: Seismic requalification of geotechnical structures. Indian Geotechnical Journal 44(2), 113-118 (2014).
7. Sarkar, R., Bhattacharya, S., Maheshwari, B. K.: Seismic requalification of pile foundations in liquefiable soils. Indian Geotechnical Journal 44(2), 183-195 (2014).
8. Seed, H. B., Idriss, I. M.: Soil moduli and damping factors for dynamic response analysis. Report EERC, 70(10) (1970).
9. Vucetic, M., Dobry, R.: Effect of soil plasticity on cyclic response. Journal of Geotechnical Engineering 117(1), 89-107 (1991).
10. Ishibashi, I., Zhang, X.: Unified dynamic shear moduli and damping ratios of sand and clay. Soils and Foundations 33, 182–191 (1993).
11. Darendeli, M.: Development of a new family of normalized modulus reduction and material damping. University of Texas (2001).
12. Vardanega, P. J., Bolton, M. D.: Stiffness of clays and silts: Normalizing shear modulus and shear strain. Journal of Geotechnical and Geoenvironmental Engineering 139(9), 1575-1589 (2013).
13. ASTM D6913/D6913M: Standard test methods for particle-size distribution (gradation) of soils using sieve analysis. ASTM International, West Conshohocken, PA (2017).
14. ASTM D4254 (2016). “Standard test methods for minimum index density and unit weight of soils and calculation of relative density.” ASTM International, West Conshohocken, PA.
15. ASTM D4253: Standard test methods for maximum index density and unit weight of soils using a vibratory table. ASTM International, West Conshohocken, PA (2016).
16. ASTM, Standard D0854: Standard test methods for specific gravity of soil solids by water pycnometer. ASTM International, West Conshohocken, PA (2014).
17. ASTM D2487: Standard practice for classification of soils for engineering purposes (Unified Soil Classification System. ASTM International, West Conshohocken, PA (2011).
18. ASTM D4015: Standard test methods for modulus and damping of soils by resonant-column. ASTM International, West Conshohocken, PA (2007).
19. ASTM D3999/D3999M: Standard test methods for the determination of the modulus and damping properties of soils using the cyclic triaxial apparatus. ASTM International, West Conshohocken, PA (2011).
20. Kumar, S. S., Krishna, A. M., Dey, A.: Evaluation of dynamic properties of sandy soil at high cyclic strains. Soil Dynamics and Earthquake Engineering 99, 157–167 (2017a).
21. Chatterjee, K., Choudhury, D: Influences of local soil conditions for ground response in kolkata city during earthquakes. In Proceedings of the National Academy of Sciences, India Section A: Physical Sciences, pp.1-14 (2016).
22. Kumar, A., Harinarayan, N. H., Baro, O.: Effects of earthquake motion and overburden thickness on strain behavior of clay and sandy soils. In Proceedings of 16th World Conference on Earthquake Engineering, pp. 9-13 (2017b).
23. Kumar, S. S., Dey, A., Krishna, A. M.: Importance of site-specific dynamic soil properties

for seismic ground response studies. International Journal of Geotechnical Earthquake Engineering 9(1), 78-98 (2018).
24. Dammala, P. K., Murali Krishna, A., Bhattacharya, S., Nikitas, G., Rouholamin, M.: Dynamic soil properties for seismic ground response studies in Northeastern India. Soil Dynamics and Earthquake Engineering 100, 357–370 (2017b).
25. Hashash, Y. M. A., Musgrouve, M. I., Harmon, J. A., Groholski, D. R., Phillips, C., Park, D.: DEEPSOIL 6.1. User Manual (2016).
26. Vucetic, M., Dobry, R.: Cyclic triaxial strain-controlled testing of liquefiable sands. In Advance Triaxial Test of Soil and Rock 475–485, (1988).
27. Kong, G., Li, H., Yang, G., Cao, Z.: Investigation on shear modulus and damping ratio of transparent soils with different pore fluids. Granular Matter 20(1), p.8 (2018).
28. Park, D., Hashash, Y. M. A.: Rate-dependent soil behavior in seismic site response analysis. Canadian Geotechnocal Journal 45, 454–469 (2008).
29. Finn, W.D.L., Bhatia, S.K.: Prediction of seismic pore water pressures. In: 10th International conference in soil mechanics and foundations. Stockholm, pp 201–206, (1982).
30. Ivsic, T.: A model for presentation of seismic pore water pressures. Soil Dynamics and Earthquake Engineerign 26, 191–199 (2006).
31. Dobry, R., Pierce, W., Dyvik, R.: Pore pressure model for cyclic straining of sand. Troy, NY (1985).
32. Seed, H.B., Martin, P.P., Lysmer, J.: The generation and dissipation of pore water pressures during soil liquefaction. Berkeley, CA (1975).
33. Chiaradonna, A., Tropeano, G., d'Onofrio, A., Silvestri, F.: Development of a simplified model for pore water pressure build-up induced by cyclic loading. Bulletin of Earthquake Engineering 1–26 (2018), doi: 10.1007/s10518-018-0354-4
34. Vucetic, M.: Cyclic Threshold Shear strains in soils. Journal of Geotechnical and Geoenvironmental Engineering 120, 2208–2228 (1995).
35. Hsu, C. C., Vucetic, M.: Volumetric Threshold shear strain for cyclic settlement. Journal of Geotechnical and Geoenvironmental Engineering 130, 58–70 (2004).
36. Dammala, P. K., Murali Krishna, A., Bhattacharya, S.. Cyclic threshold shear strains in cohesionless soils based on stiffness degradation. In Proceeding of Indian Geotechnical Conference, Pune, Maharastra, India (2015).
37. Heshmati, A. A., Shahnazari, H., Sarbaz, H.: The cyclic threshold shear strains in very dense clean sand. Europian Journal of Environmental and Civil Engineering 19, 884–899 (2015).
38. Chattaraj, R., Sengupta, A.: Liquefaction potential and strain dependent dynamic properties of Kasai River sand. Soil Dynamics and Earthquake Engineering, 90, 467–475 (2016).
39. Chung, R. M., Yokel, F. Y., Drnevich, V. P.: Evaluation of dynamic properties of sands by resonant column testing. Geotechnical Testing Journal **7**, 60-69 (1984).
40. Dutta, T. T., Saride, S.: Dynamic properties of clean sand from resonant column. In Proceeding of Indian Geotechnical Conference, Kakinada, India (2014).
41. Govindaraju, L.: Liquefaction and dynamic properties of sandy soils. PhD Thesis, Submitted to Indian Institute of Science Bangalore (2005).
42. HanumanthaRao, C., Ramana, G. V.: Dynamic soil properties for microzonation of Delhi. Journal of Earth System and Science, 117, 719–730 (2008).
43. Kirar, B., Maheswari, B.: Effects of silt content on dynamic properties of solani sand. In Proceeding of 7th International Conference on Case History in Geotechnical Engineeirng, pp. 1–7 (2013).
44. Kumar, J., Achu, C. C.: Effect of cyclic strain history on shear modulus of dry sand using resonant column tests. Geotechnical Engineering Journal of SEAGS, AGSSEA 46 99–104 (2014).